Unidentate and Bidentate Binding of Nickel(II) Complexes to an Fe_4S_4 Cluster *via* Bridging Thiolates: Synthesis, Crystal Structures, and Electrochemical Properties of Model Compounds for the Active Sites of Nickel Containing CO Dehydrogenase/Acetyl-CoA Synthase

Frank Osterloh, Wolfgang Saak,* and Siegfried Pohl†

Contribution from the Department of Chemistry, University of Oldenburg, 26111 Oldenburg, Germany

Received January 21, 1997[⊗]

Abstract: $[Ni(EtN_2S_2)]$ (**1**) (EtN_2S_2 = *N*,*N*′-diethyl-3,7-diazanonane-1,9-dithiolate) and $[Ni(S_4)]$ (**2**) (S_4 = 3,7-dithianonane-1,9-dithiolate) react with $[Fe_4S_4I_4]^{2-}$ to afford the neutral clusters $[\{Ni(EtN_2S_2)\}_2Fe_4S_4I_2]$ (**3**) and $[\{Ni(S_4)\}_2Fe_4S_4I_2]$ (**4**), respectively. Metathesis with potassium arenethiolates yields the clusters $[\{Ni(EtN_2S_2)\}_2Fe_4S_4(Stip)_2]$ (**5**) and $[\{Ni(S_4)\}_2Fe_4S_4(Stip)_2]$ (**6**) (tip = 2,4,6-triisopropylbenzene). Alternatively, the latter compounds can be synthesized by action of the corresponding Ni complexes on $[Fe_4S_4(Stip)_2L_2]$ (L = 2,3-dimethyl-1-phenyl-3-pyrazoline-5-thione), where the neutral ligands are displaced by the Ni complexes. As elucidated by single-crystal X-ray crystallography, **3**, **5**, and **6** are composed of an $[Fe_4S_4]^{2+}$ unit and two Ni(II) complexes and the Ni and Fe centers are bridged *via* one and two μ_2-sulfur atoms from either the EtN_2S_2 or the S_4 ligands. In **3** and **5** two N and two S (thiolate) atoms serve as donors for a square planar coordinated Ni(II) ion, whereas **6** contains two Ni(II) ions in a square planar S_2 (thioether) S_2 (thiolate) environment. The structures of the NiFe heterometallic clusters are discussed and related to the structures of the active sites of Ni containing CO dehydrogenases/acetyl-CoA synthases. As demonstrated by ^{1}H-NMR spectroscopy, **3**, **5**, and **6** retain their bridged structures in solution. However, the spectra of **5** and **6** can be interpreted in terms of a symmetrical bidentate coordination of both Fe_4S_4-bound Ni complex fragments, which would be in contrast to the unidentate (**5**) or unsymmetrically bidentate (**6**) binding observed in the solid state. The redox properties of clusters **3**, **5**, and **6** were determined by cyclic voltammetry. In dichloromethane solution **5** exhibits two quasi-reversible oxidation processes at 0 and +485 mV and one quasi-reversible reduction wave at −1050 mV (*vs* SCE).

Introduction

The metabolism of certain acetogenic and methanogenic bacteria is dependent on nickel−carbon monoxide dehydrogenase (CODH)/acetyl-CoA synthase (ACS), one of only four Ni-containing enzymes[1] presently known. Elemental analyses have shown the enzyme from *Clostridium thermoaceticum* to contain 2 Ni, 11−13 Fe, and 14 S in the form of sulfide.[2] These elements constitute three centers of unknown structure that are believed to be the catalytic components of Ni−CODH/ACS.[3,4] Acetyl-CoA assembly from carbon monoxide, coenzyme A, and a methyl group from a corrinoid iron−sulfur protein is catalyzed by center A (reaction 1), whereas center C is responsible for CO oxidation (reaction 2). Ni−CODHs from photosynthetic bacteria lack center A and therefore only catalyze CO oxidation. Center B is thought to be a conventional Fe_4S_4 cluster with electron transport function.

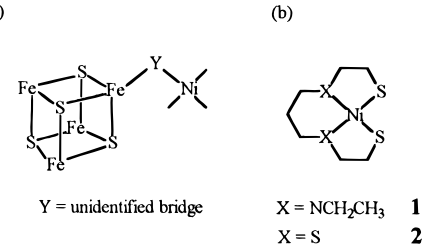

Figure 1. (a) Proposed structure of the Ni−Y−Fe_4S_4 assembly of center A of CO dehydrogenase (according to ref 5). (b) Structure of $[Ni(EtN_2S_2)]$ (**1**) and $[Ni(S_4)]$ (**2**).

$$\text{center A:}\quad CO + CH_3^+ + CoA{-}S^- \rightarrow CoA{-}SC(O)CH_3 \qquad (1)$$

$$\text{center C:}\quad CO + H_2O \rightleftharpoons CO_2 + 2H^+ + 2e^- \qquad (2)$$

Figure 1a illustrates a proposed structural model for center A.[1,4−6] It consists of a Fe_4S_4 cubane cluster covalently linked to a mononuclear Ni center *via* a common ligand Y. The bridging ligand Y has not yet been identified, but it seems to

* To whom correspondence should be addressed.

† Deceased.

⊗ Abstract published in *Advance ACS Abstracts,* June 1, 1997.

(1) (a) *Bioinorganic Chemistry: Inorganic Elements in the Chemistry of Life*; Kaim, W., Schwederski, B., Eds.; Wiley: New York, 1995. (b) Kolodziej, A. F. *Prog. Inorg. Chem.* **1994**, *41*, 493. (c) *The Bioinorganic Chemistry of Nickel*; Lancaster, J. R., Ed.; VCH: New York, 1988. (d) Halcrow, M. A.; Christou, G. *Chem. Rev.* **1994**, *94*, 2421. (e) Cammack, R. In *Bioinorganic Catalysis*; Reedijk, J., Ed.; Marcel Dekker: New York, 1993; pp 189−225.

(2) (a) Ragsdale, S. W.; Clark, J. E.; Ljungdahl, L. G.; Lundie, H. L.; Drake, H. L. *J. Biol. Chem.* **1983**, *258*, 2364. (b) Lindahl, P. A.; Ragsdale, S. W.; Münck, E. *J. Biol. Chem.* **1990**, *265*, 3880.

(3) (a) Seravalli, J.; Kumar, M.; Lu, W. -P.; Ragsdale, S. W. *Biochemistry* **1995**, *34*, 7879. (b) Kumar, M.; Lu, W. -P.; Liu, L.; Ragsdale, S. W. *J. Am. Chem. Soc.* **1993**, *115*, 11646.

(4) (a) Kumar, M.; Qiu, D.; Spiro, T. G.; Ragsdale, S. W. *Science* **1995**, *270*, 628. (b) Ragsdale, S. W.; Kumar, M. *Chem. Rev.* **1996**, *96*, 2515. (c) Ragsdale, S. W.; Riordan, C. G. *JBIC* **1996**, *1*, 489.

(5) Qiu, D.; Kumar, M.; Ragsdale, S. W.; Spiro, T. G. *Science* **1994**, *264*, 817.

(6) Tucci, G. C.; Holm, R. H. *J. Am. Chem. Soc.* **1995**, *117*, 6489.

S0002-7863(97)00194-7 CCC: $14.00

be a μ_2-bridging thiolate residue or μ_2-sulfide. Although convincing evidence is still lacking, center C, the CO oxidation site, is believed to have closely related structure.[7,8] Differences between both centers may in part arise from different coordination environments of the Ni ions. Whereas center A from *C. thermoaceticum* exhibits spectroscopic properties that implicate a distorted square planar Ni coordination sphere of two S donors at 219 pm and two N/O donors at 189 pm,[9] the Ni environment of center C, as studied by XAS on *Rhodospirillum rubrum*, is proposed to be distorted tetrahedral or five-coordinate with 2 S atoms at 223 pm and 2−3 N/(O) atoms at 187 pm.[8]

Though functional aspects of the active centers have been successfully modeled with simple Ni coordination compounds,[6,10−13] there is still no structural model available for the proposed μ_2-S(thiolate)-bridged assembly of the Fe_4S_4 unit and Ni ion. This is in part due to the chemistry of Ni(II) thiolate complexes, in which the Ni(II)-bound thiolate function has a high tendency to form μ_2-thiolate-bridged polynuclear assemblies—a behavior that often complicates the aimed synthesis of a complex of definite composition. However, in Ni(II) complexes, in which two Ni coordination sites are blocked by nonbridging atoms, *e.g.*, N or thioether S, the formation of bridged assemblies can be controlled. $[Ni(S_4)]$ and $[Ni(N_2S_2)]$ (Figure 1b) and derivatives, which contain Ni(II) in square planar environments of thioether S and thiolate S[14,15] or N and thiolate S donors,[16−23] respectively, are known to exist in either mononuclear or polynuclear form. The latter are formed by action of the mononuclear complexes on additional metal ions, to which they bind *via* one or two μ_2-thiolate(s).[24−26] Accordingly, on reaction with Fe_4S_4 clusters, bridged assemblies are formed, in which the iron atoms of the Fe_4S_4 core are covalently linked to the Ni centers by the S atoms of the chelating ligands. We report here the syntheses and the solid state structures of some of the resulting $Ni(\mu_2\text{-}SR)[Fe_4S_4]$ clusters, and of their products of metathesis with arenethiolates, their ^{1}H-NMR spectra, and their electrochemical properties. The crystal structure for **3** has been previously communicated.[27]

Experimental Section

Preparation of Compounds. Unless noted otherwise, all operations were carried out at room temperature under a pure nitrogen atmosphere by using glove boxes and Schlenk techniques. Tetrahydrofurane (THF) and ether were distilled from Na/K, dichloromethane was distilled from CaH_2, and acetonitrile was distilled from P_4O_{10}. *N*,*N*′-Diethyl-1,3-diaminopropane (97%), ethylenesulfide (98%) and tetra-n-butylammoniumhexafluorophosphate (>99%) were of commercial quality and used as received. Nickelacetylacetonate (98%) was recrystallized from THF to remove insoluble impurities. 2,4,6-Tri(isopropyl)benzenethiol (HStip) was obtained by $LiAlH_4$ reduction of the commercially available sulfochloride. The K^+ salt is available by reaction of potassium metal with the free thiol in THF solution. 3,7-Dithianonane-1,9-dithiol (S_4H_2) was synthesized according to literature methods,[28] and $[Fe_4S_4(Stip)_2(tap)_2]$ (tap = thioantipyrine = 2,3-dimethyl-1-phenyl-3-pyrazoline-5-thione) was prepared according to Harmjanz et al.[29] $(BTBA)_2[Fe_4S_4I_4]\cdot$THF (BTBA = Benzyltri(n-butyl)ammonium) was synthesized by a modified procedure for the benzyltri(methyl)ammonium salt.[30]

***N*,*N*′-Diethyl-3,7-diazanonane-1,9-dithiol [modified procedure from ref 31].** Solutions of 9.11 mL (57.3 mmol) of *N*,*N*′-diethyl-1,3-diaminopropane in 20 mL of toluene and 7.46 mL (125 mmol) of ethylene sulfide (10% excess) in 20 mL of the same solvent were mixed at room temperature and heated to 110 °C in a sealed tube for 24 h. After being cooled to room temperature, the solution was filtered to remove a small amount of insoluble material. The solvent was evaporated under reduced pressure, leaving the product as a colorless oil of >95% purity, judged by ^{13}C-NMR spectroscopy (the crude product proved to be sufficient for the synthesis of the corresponding Ni complex). Distillation over a small column (124−129 °C; 0.1 mbar) gave the pure product as a colorless liquid. Yield: 12.9 g (51.6 mmol), 90%. ^{1}H-NMR (300 MHz, $CDCl_3$) [ppm]: 0.97 (t, 6H), 1.53 (quintet, 2H), 1.69 (s, 2H), 2.48 (m, 16H). ^{13}C-NMR (75.5 MHz, $CDCl_3$) [ppm]: 11.73, 22.65, 24.91, 47.16, 51.21, 56.35.

[*N*,*N*′-Diethyl-3,7-diazanonane-1,9-dithiolato]nickel(II) [$Ni(EtN_2S_2)$] (1). A 1.00 g (4.00 mmol) sample of *N*,*N*′-diethyl-3,7-diazanonane-1,9-dithiol was added to a stirred solution of 1.03 g (4.00 mmol) of nickel acetylacetonate in 20 mL of THF. Immediately the color changed from green to red-brown. When the reaction mixture was kept at room temperature for 24 h, a purple microcrystalline solid formed, which was filtered off, washed with THF, and dried *in vacuo*. Yield: 1.00 g (3.26 mmol), 81%. IR (KBr): 3019 vw, 3005 w, 2988 m, 2944 s, 2922 s, 2876 s, 2847 vs, 2812 w, 1481 m, 1460 s, 1433 s, 1418 m, 1397 m, 1368 w, 1354 m, 1331 s, 1304 s, 1279 vw, 1256 s, 1217 w, 1204 s, 1192 s, 1150 m, 1134 m, 1105 m, 1061 s, 1040 s,

(7) Hu, Z.; Spangler, N. J.; Anderson, M. E.; Xia, J.; Ludden, P. W.; Lindahl, P. A.; Münck, E. *J. Am. Chem. Soc.* **1996**, *118*, 830.
(8) Tan, G. O.; Ensign, S. A.; Ciurli, S.; Scott, M. J.; Hedman, B.; Holm, R. H.; Ludden, P. W.; Korszun, Z. R.; Stephens, P. J.; Hodgson, K. O. *Proc. Natl. Acad. Sci. U.S.A.* **1992**, *89*, 4427.
(9) Xia, J. Q.; Dong, J.; Wang, S. K.; Scott, R. A.; Lindahl, P. A. *J. Am. Chem. Soc.* **1995**, *117*, 7065.
(10) (a) Stavropoulos, P.; Muetterties, M. C.; Carrie, M.; Holm, R. H. *J. Am. Chem. Soc.* **1991**, *113*, 8485. (b) Stavropoulos, P.; Carrie, M.; Muetterties, M. C.; Holm, R. H. *J. Am. Chem. Soc.* **1990**, *112*, 5385.
(11) Sellmann, D.; Häussinger, D.; Knoch, F.; Moll, M. *J. Am. Chem. Soc.* **1996**, *118*, 5368.
(12) Hillhouse, G. L.; Matsunaga, P. T. *Angew. Chem.* **1994**, *106*, 1841; *Angew. Chem., Int. Ed. Engl.* **1994**, *33*, 1748.
(13) Ram, M. S.; Riordan, C. G.; Yap, G. P. A.; Liable-Sands, L.; Rheingold, A. L.; Marchaj, A.; Norton, J. R. *J. Am. Chem. Soc.* **1997**, *119*, 1648.
(14) Yamamura, T.; Arai, H.; Nakamura, N.; Miyamae, H. *Chem. Lett.* **1990**, 2121.
(15) (a) Yamamura, T.; Sakurai, S.; Arai, H.; Miyamae, H. *J. Chem. Soc., Chem. Commun.* **1993**, 1656. (b) Roundhill, D. M. *Inorg. Chem.* **1980**, *19*, 557.
(16) Colpas, G. J.; Kumar, M.; Day, R. O.; Maroney, M. J. *Inorg. Chem.* **1990**, *29*, 4779.
(17) Turner, M. A.; Driessen, W. L.; Reedijk, J. *Inorg. Chem.* **1990**, *29*, 3331.
(18) Drew, M. G. B.; Rice, D. A.; Richards, K. M. *J. Chem. Soc., Dalton Trans.* **1980**, 2075.
(19) Tuntulani, T.; Reibenspies, J. H.; Farmer, P. J.; Darensbourg, M. Y. *Inorg. Chem.* **1992**, *31*, 3497.
(20) (a) Jicha, D. C.; Busch, D. H. *Inorg. Chem.* **1962**, *1*, 872. (b) Jicha, D. C.; Busch, D. H. *Inorg. Chem.* **1962**, *1*, 878. (c) Root, C. A.; Busch, D. H. *Inorg. Chem.* **1968**, *7*, 789. (d) Girling, R. L.; Amma, E. L. *Inorg. Chem.* **1967**, *6*, 2009. (e) Wei, C. H.; Dahl, L. F. *Inorg. Chem.* **1970**, *9*, 1878. (f) Kang, D.-X.; Poor, M.; Blinn, E. L.; Treichel, P. M. *Inorg. Chim. Acta* **1990**, *168*, 209. (g) Farmer, P. J.; Solouki, T.; Mills, D. K.; Soma, T.; Russell, D. H.; Reibenspies, J. H.; Darensbourg, M. Y. *J. Am. Chem. Soc.* **1992**, *114*, 4601. (h) Darensbourg, M. Y.; Tuntulani, T.; Reibenspies, J. H. *Inorg. Chem.* **1995**, *34*, 6287. (i) Maroney, M. J.; Choudhury, S. B.; Bryngelson, P. A.; Mirza, S. A.; Sherrod, M. J. *Inorg. Chem.* **1996**, *35*, 1073. (j) Mills, D. K.; Reibenspies, J. H.; Darensbourg, M. Y. *Inorg. Chem.* **1990**, *29*, 4364.
(21) Musie, G.; Farmer, P. J.; Tuntulani, T.; Reibenspies, J. H.; Darensbourg, M. Y. *Inorg. Chem.* **1996**, *35*, 2176.
(22) Wei, C. H.; Dahl, L. F. *Inorg. Chem.* **1970**, *9*, 1878.
(23) Baidya, N; Ndreu, D; Olmstead, M. M., Mascharak, P. K. *Inorg. Chem.* **1991**, *30*, 2448.
(24) Some recent examples of bridged assemblies include the tetrametallic $[Fe\{Ni(N_2S_2)\}_3]^{2+}$, in which a central Fe(II) ion is bound to three $[Ni(N_2S_2)]$ complexes *via* μ_2-S thiolates[25] and $[\{Ni(N_2S_2)\}Fe(CO)_4]$ in which one $[Ni(N_2S_2)]$ complex and an $Fe(CO)_4$ fragment are bridged *via* one μ_2-S atom of the chelating N_2S_2 ligand.[26]
(25) Colpas, G. J.; Day, R. O.; Maroney, M. J. *Inorg. Chem.* **1992**, *31*, 5053.
(26) C.-H. Lai, J. H. Reibenspies, M. Y. Darensbourg, *Angew. Chem.* **1996**, 108, 2551; *Angew. Chem., Int. Ed. Engl.* **1996**, *35*, 2390.
(27) Osterloh, F.; Saak, W.; Haase, D.; Pohl, S. *Chem. Commun.* **1996**, 777.
(28) Rosen, W.; Busch, D. H. *J. Am. Chem. Soc.* **1969**, *91*, 4694.
(29) Harmjanz, M.; Junghans, C.; Opitz, U. -A.; Bahlmann, B.; Pohl, S. *Z. Naturforsch.* **1996**, *51b*, 1040.
(30) Saak, W.; Pohl S. *Z. Naturforsch.* **1985**, *40b*, 1105. The cluster was obtained as a THF solvate by a modified procedure: Benzyltri-*n*-butylammonium iodide was used instead of benzyltrimethylammonium iodide, and the reaction mixture, after being refluxed for 12 h, was not taken to dryness *in vacuo*, but was cooled to room temperature and stored overnight to afford the crystalline product. The crystals were filtered off, washed with THF, and dried *in vacuo*.
(31) Corbin, J. L.; Miller, K. F.; Pariyadath, N.; Wherland, S.; Bruce, A. E.; Stiefel, E. I. *Inorg. Chim. Acta* **1984**, *90*, 41.

1032 s, 995 s, 970 vs, 941 s, 912 s, 868 m, 781 vs, 750 vs, 689 w, 557 w, 548 w, 530 w, 509 m, 449 m, 382 s, 353 m, 289 w cm^{-1}. Anal. Calcd for $C_{11}H_{24}N_2NiS_2$: C, 43.02; H, 7.88; N, 9.12; S, 20.88. Found: C, 43.55; H; 8.04; N, 9.10; S, 20.84. UV/vis spectrum (CH_3CN): λ_{max} 640 (20), 480 (115), 360 (140) nm (M^{-1} cm^{-1}). ^{1}H-NMR (500 MHz, CD_3CN) [ppm]: 0.89 (t, 6H, CH_3), 1.43 (m, 2H, CH_2-CH_2CH_2), 1.52 (m, 1H, CH_2C$H_2$$CH_2$), 1.74 (m, 1H, CH_2C$H_2$$CH_2$), 1.97 (m, 2H, C$H_2$$CH_2CH_2$), 2.56 (m, 6H, SC$H_2$$CH_2$N + NC$H_2$$CH_2$S), 2.86 (m, 2H, NC$H_2$$CH_2$S), 3.36 (m, 2H, CH_3CH_2), 3.67 (m, 2H, CH_3CH_2) (see also Figure 6).

[3,7-Dithianonane-1,9-dithiolato]nickel(II) [Ni(S$_4$)] (2). To a stirred solution of 4.50 g (18.9 mmol) of $NiCl_2$·$6H_2O$ in 100 mL of water and 60 mL of ethanol was added a solution of 4.50 g (19.7 mmol) of S_4H_2 and 18 mL of 17.5% NaOH (78.8 mmol) in 50 mL of water at 50 °C. The resultant brown solution was refluxed for 30 min and filtered while hot. Storage of the filtrate at 5 °C afforded 4.50 g (15.8 mmol), 80%, of black needles, which were collected by filtration after 24 h, washed with ethanol, and dried *in vacuo*. IR (KBr): 2974 vw, 2944 w, 2918 m, 2897 m, 2880 s, 2818 m, 1439 m, 1424 s, 1416 vs, 1406 m, 1290 s, 1273 s, 1258 s, 1238 s, 1186 w, 1155 w, 1148 w, 1123 w, 1099 m, 1082 m, 1047 m, 1013 w, 991 w, 932 m, 918 m, 868 s, 849 vs, 831 s, 681 vw, 669 vw, 652 vw, 457 m, 386 m, 320 s, 297 m cm^{-1}. Anal. Calcd for $C_7H_{14}NiS_4$: C, 29.94; H, 4.95; S, 44.98. Found: C, 29.47; H, 4.94; S, 45.24. UV/vis spectrum (CH_3OH): λ_{max} 610 (35), 510 (105), 425 (270), 370 (240) nm (M^{-1} cm^{-1}). ^{1}H-NMR (500 MHz, DMSO-d_6) [ppm]: 1.64 (m, 1H, CH_2C$H_2$$CH_2$), 2.08 (s, 2H), 2.22 (s, 2H), 2.60 (s, 3H, CH_2C$H_2$$CH_2$ + ?), 2.89 (s, 2H), 3.10 (s, 2H), 3.45 (s, 2H).

[{Ni(EtN$_2$S$_2$)}$_2$Fe$_4$S$_4$I$_2$] (3)·2CH$_3$CN. To a solution of 0.500 g (1.63 mmol) of **1** in 20 mL of CH_3CN was added a solution of 1.20 g (0.814 mmol) of $(BTBA)_2[Fe_4S_4I_4]$·THF in 25 mL of CH_3CN with stirring. When the black reaction mixture was kept at room temperature for 24 h, the product crystallized as black needles. The crystals were filtered off, washed with acetonitrile to remove benzyltributylammonium iodide, and dried *in vacuo*. Yield: 1.00 g (0.768 mmol), 94%. The product contains two molecules of acetonitrile per formula. Single crystals of **3**·2CH_3CN were obtained following the above procedure and using a 1:1 mixture of CH_2Cl_2 and CH_3CN instead of pure CH_3CN as solvent. IR (KBr): ν(CH_3CN) = 2245 w cm^{-1}; ν(Fe_4S_4) = 380 s, 361 m, 280 s cm^{-1}. Anal. Calcd for $C_{26}H_{54}Fe_4I_2N_6Ni_2S_8$: C, 23.99; H, 4.18; N, 6.46; S, 19.70. Found: C, 24.10; H, 4.24; N, 6.57; S, 20.02. UV/vis spectrum (CH_2Cl_2): λ_{max} 495 (11 200), 380 (18 500), 265 (48 200) nm (M^{-1} cm^{-1}). ^{1}H-NMR (300 MHz, CD_2Cl_2) [ppm]: −1.90 (s, 4H, NC$H_2$$CH_2$S), −0.02 (s, 4H, NC$H_2$$CH_2$S), 0.54 (s, 2H, CH_2C$H_2$$CH_2$), 1.14 (s, 12H, C$H_3$), 1.59 (s, 4H, C$H_2$$CH_2CH_2$), 2.04 (s, 4H, C$H_2$-$CH_2CH_2$), 2.00 ($CH_3CN$), 2.39 (s, 2H, CH_2C$H_2$$CH_2$), 4.19 (m, 8H, C$H_2$-$CH_3$), 16.76 (s, 4H, SC$H_2$), 18.96 (s, 4H, SC$H_2$) (see also Figure 6).

[{Ni(S$_4$)}$_2$Fe$_4$S$_4$I$_2$] (4)·THF. To a solution of 0.500 g (1.75 mmol) of **2** in 20 mL of CH_2Cl_2 was added a solution of 1.30 g (0.877 mmol) of $(BTBA)_2[Fe_4S_4I_4]$·THF in 25 mL of the same solvent with stirring. The product precipitated spontaneously as a microcrystalline solid, which was filtered off after 5 min, washed with 20 mL of CH_2Cl_2 to remove benzyltributylammonium iodide, and dried *in vacuo*. Yield: 1.00 g (0.850 mmol), 97%. IR (KBr): ν(Fe_4S_4) = 380 s cm^{-1}. Anal. Calcd for $C_{18}H_{36}Fe_4I_2Ni_2OS_{12}$ (THF possibly stems from $(BTBA)_2$-$[Fe_4S_4I_4]$·THF): C, 17.33; H, 2.91; S, 30.83. Found: C, 17.59; H, 2.90; S, 30.77. UV/vis spectrum (1,2-propylene carbonate): λ_{max} 405 (12 200), 305 (27 600) nm (M^{-1} cm^{-1}). The cluster is only soluble in 1,2-propylene carbonate and 1,3-dimethylimidazolidin-2-one.

[{Ni(EtN$_2$S$_2$)}$_2$Fe$_4$S$_4$(Stip)$_2$] (5)·THF. Method A. To a stirred suspension of 400 mg (307 μmol) of **3** in 20 mL of CH_3CN was added 170 mg (619 μmol) of solid potassium 2,4,6-triisopropylbenzenethiolate, resulting in a black solution. Stirring was continued until the supernatant solution became almost colorless and a black solid had formed (24 h). The solvent was evaporated *in vacuo*, and 20 mL of THF was added to the solid residue, resulting in precipitation of KI and dissolution of the product. The suspension was filtered, and the volume of the filtrate was reduced to 50% *in vacuo*. When the filtrate was stored at room temperature the analytically pure product precipitated as black crystals, suitable for X-ray crystallography. The crystals were filtered off after 24 h, washed with small amounts of THF, and dried *in vacuo* to afford 390 mg (271 μmol), 88%. **5** can be obtained as an acetonitrile solvate when a solution of **5** in THF is taken to dryness *in vacuo* and 20 mL of acetonitrile is added to the solid residue. A black solution forms, from which black needles crystallize during 12 h in almost quantitative yield. IR (KBr): ν(Fe_4S_4) = 378 m, 339 s cm^{-1}. Anal. Calcd for $C_{56}H_{102}Fe_4N_4Ni_2OS_{10}$: C, 44.58; H, 6.81; N, 3.71; S, 21.25. Found: C, 44.80; H, 6.81; N, 3.70; S, 21.13 (the sample for elemental analysis was not dried *in vacuo*). UV/vis spectrum (CH_2-Cl_2): λ_{max} 428 (19 400), 280 (39 500), 240 (51 500) nm (M^{-1} cm^{-1}). ^{1}H-NMR (500 MHz, $CDCl_3$) [ppm]: −0.20 (s, 4H), 0.69 (s, 4H), 1.06 (s, 12H), 1.12 (s, 12H, *p*-CH_3), 1.66 (s, 24H, *o*-CH_3), 2.00 (s, 4H), 2.38 (s, 2H, CH_2C$H_2$$CH_2$), 3.37 (s, 2H, *p*-CH), 3.97 (s, 8H, CH_3CH_2), 5.32 (s, 4H, *o*-CH), 8.25 (s, 4H, Ar-H), 12.76 (s, 4H, SCH_2), 15.26 (s, 4H, SCH_2) (see also Figure 6).

Method B. To a stirred suspension of 80 mg (65 μmol) of $[Fe_4S_4(Stip)_2(tap)_2]$ in 5 mL of CH_3CN was added a solution of 40 mg (130 μmol) of **1** in 2 mL of the same solvent. A red-black solution was obtained, from which the analytically pure product crystallized within 12 h. The needle-shaped crystals were filtered off, washed with small portions of CH_3CN, and dried *in vacuo* to give 75 mg (52 μmol), 80%, of product, identical with the acetonitrile solvate of **5** obtained by method A.

[{Ni(S$_4$)}$_2$Fe$_4$S$_4$(Stip)$_2$] (6). Method A. A suspension of 400 mg (340 μmol) of **4** and 200 mg (730 μmol) of potassium 2,4,6-triisopropylbenzenethiolate in 20 mL of CH_2Cl_2 was stirred for 12 h. The black reaction mixture was filtered to remove KI, and 20 mL of ether was added to the filtrate. Within 20 h the product crystallized as black needles, which were filtered off, washed with ether/CH_2Cl_2 (1:1), and dried *in vacuo*. Yield: 260 mg (176 μmol), 52%. Crystals suitable for X-ray crystallography were grown from concentrated solutions of **6** in dichloromethane. IR (KBr): ν(Fe_4S_4) = 365 m, 336 s cm^{-1}. Anal. Calcd for $C_{44}H_{74}Fe_4Ni_2S_{14}$: C, 37.95; H, 5.36; S, 32.23. Found: C, 37.24; H, 5.24; S, 32.30. UV/vis spectrum (CH_2Cl_2): λ_{max} 416 (18 600), 285 (38 300), 245 (49 400) nm (M^{-1} cm^{-1}). ^{1}H-NMR (300 MHz, $CDCl_3$) [ppm]: 0.92 (s, 4H), 1.15 (s, 12H, p-CH(CH_3)$_2$), 1.22 (s, 4H), 1.64 (s, 24H, *o*-CH(CH_3)$_2$), 2.40 (s, 4H), 2.57 (s, 4H), 3.26 (s, 2H, *p*-CH(CH_3)$_2$), 3.26 (s, 4H), 5.28 (s, 4H, *o*-CH(CH_3)$_2$), 8.29 (s, 4H, Ar-H), 9.06 (s, 8H, SCH_2) (see also Figure 6).

Method B. To a suspension of 65 mg (53 μmol) of $[Fe_4S_4(Stip)_2(tap)_2]$ in 1 mL of CH_2Cl_2 was added a solution of 30 mg (105 μmol) of **2** in 2 mL of CH_2Cl_2 with stirring. Immediately, a clear brown solution formed, which was stirred for an additional 10 min and then filtered to remove a small amount of insoluble material. A 2 mL portion of ether was added to the filtrate, and the solution was kept at room temperature. Within 12 h the product crystallized as black needles, which were filtered off, washed with ether/CH_2Cl_2 (1:1), and dried *in vacuo* to afford 60 mg (41 μmol), 78%, of product, which proved to by identical with that obtained by method A.

X-ray Structure Determinations. Crystal and data collection parameters for **3**, **5**, and **6** are summarized in Table 1 together with refinement parameters. Single crystals of the compounds were obtained as described in the preparative section.

[{Ni(EtN$_2$S$_2$)}$_2$Fe$_4$S$_4$I$_2$] (**3**) crystallizes as a solvate with two molecules of acetonitrile per formula. A black single crystal (0.68 × 0.57 × 0.42 mm) of **3**·2CH_3CN was sealed in a glass capillary and mounted on a Siemens-Stoe AED 2 four-circle diffractometer. Data collection using Mo Kα radiation (λ = 71.073 pm) and ω−2θ scans gave 2273 independent reflections (θ_{max} = 26°), of which 1870 with $I > 2\sigma(I)$ were used in all calculations. A semiempirical absorption correction using Ψ scans was applied. The structure was solved by direct methods and the solution developed using full-matrix least-squares refinement on F^2 and difference Fourier synthesis.[32] Anisotropic displacement parameters were refined for all non-H atoms. H atoms were included on calculated positions with isotropic displacement parameters tied to those of the corresponding carbon atoms. At convergence, R = 0.0353, wR_2 = 0.0655, and GOF = 1.067 for 217 parameters.

A black prism-shaped crystal (0.59 × 0.48 × 0.38 mm) of [{Ni-(EtN$_2$S$_2$)}$_2$Fe$_4$S$_4$(Stip)$_2$] (**5**)·THF was sealed in a glass capillary employing a THF atmosphere to prevent loss of THF. Data collection, which was performed according to the above described procedures, gave 6289 independent reflections (θ_{max} = 23°), of which 5223 with $I > 2\sigma(I)$ were used in all calculations. No absorption correction was

(32) Sheldrick, G. M., Göttingen, FRG, 1990, 1993.

Table 1. Crystal and Data Collection Parameters for **3**·2CH_3CN, **5**·THF, and **6**·3CH_2Cl_2

compound	**3**	**5**	**6**
formula	$C_{26}H_{54}Fe_4I_2N_6Ni_2S_8$	$C_{56}H_{102}Fe_4N_4Ni_2OS_{10}$	$C_{47}H_{80}Cl_6Fe_4Ni_2S_{14}$
fw	1301.86	1508.84	1647.47
crystal system	tetragonal	orthorhombic	monoclinic
space group	$I4_1cd$	$P2_12_12_1$	$P2_1/n$
a (pm)	2088.8(1)	1497.5(1)	1818.4(2)
b (pm)	2088.8(1)	1947.3(1)	1323.4(1)
c (pm)	2053.2(1)	2824.2(2)	2910.2(4)
β (deg)			93.21(2)
V (nm^3)	8.9583(7)	8.2356(9)	6.9923(13)
Z	8	4	4
ρ_{calc} (g/cm^{-3})	1.931	1.217	1.565
μ (mm^{-1})	3.864	1.420	2.014
crystal dimns (mm)	0.68 × 0.57 × 0.42	0.59 × 0.48 × 0.38	0.80 × 0.48 × 0.17
no. of data collected[a]	4445	6289	10 221
no. of unique data	2273	6289	9709
data [$I > 2\sigma(I)$]	1870	5223	7797
$R1$[b] [$I > 2\sigma(I)$]	0.0353	0.0761	0.0971
wR_2[c] [$I > 2\sigma(I)$]	0.0655	0.1921	0.1914

[a] Collected at 296(2) K using Mo Kα (λ = 71.073 pm) radiation. [b] $R_1 = \sum||F_o| - |F_c||/\sum|F_o|$. [c] $wR_2 = \{\sum[w(F_o^2 - F_c^2)^2]/[w(F_o^2)^2]\}^{1/2}$.

applied. The structure was solved by direct methods; full-matrix least-squares refinement was on F^2.[32] Anisotropic displacement parameters were refined for all non-H atoms; H atoms were treated as described for **3**. THF was refined with idealized geometry. At convergence, R = 0.0761, wR_2 = 0.1921, and GOF = 1.262 for 645 parameters.

A suitable black platelike crystal (0.80 × 0.48 × 0.17 mm) of [{Ni(S$_4$)}$_2$$Fe_4S_4$(Stip)$_2$] (**6**)·3$CH_2Cl_2$ was sealed in a glass capillary under a CH_2Cl_2 atmosphere to prevent loss of the crystal solvent. Intensity data collections were performed according to **3** and **5**. A semiempirical absorption correction using Ψ scans was applied to 10 221 reflections (θ_{max} = 23°). A total of 7797 unique reflections with $I > 2\sigma(I)$ were used in further calculations. The structure was solved by direct methods [SHELXS, SHELXTL-PLUS][32] with full-matrix least-squares anisotropic refinement for all non-hydrogen atoms. Hydrogen atoms were treated as described for **3**. The three CH_2Cl_2 molecules in the asymmetric unit were all disordered. Refinement with idealized geometry on two positions with occupancy factors of 0.5 led to satisfactory results. Three of the isopropyl groups and one ethylene group of the tetradentate ligand were treated in the same way. No H positions were calculated at the disordered carbon atoms. At convergence, R = 0.0971, wR_2 = 0.1914, and GOF = 1.280 for 619 parameters.

Other Physical Measurements. All measurements were made under strictly anaerobic conditions. $^1H/^{13}C$-NMR spectra were recorded with Bruker AMX 500 and AM 300 spectrometers and referenced to solvent signals or TMS as internal standard. IR and UV/vis spectra were recorded with a Biorad FTS-7 and a Shimadzu UV-260 spectrometer, respectively. Cyclic voltammograms were recorded using Pt electrodes, a SCE for reference, and 0.1 M (n-Bu_4N)PF_6 as supporting electrolyte.

Results and Discussion

Synthetic Studies. The complexes [*N*,*N*′-diethyl-3,7-diazanonane-1,9-dithiolato]nickel(II) (**1**) and [3,7-dithianonane-1,9-dithiolato]nickel(II) (**2**), which contain Ni(II) in square planar N_2S_2 and S_4 coordination environments, respectively, react smoothly with (BTBA)$_2$[$Fe_4S_4I_4$] (BTBA = benzyltri-*n*-butylammonium) to form the neutral $Ni_2Fe_4S_4$ clusters **3** and **4** (Figure 2). In the bridged assemblies [{Ni(EtN_2S_2)}$_2$$Fe_4S_4I_2$] (**3**) and [{Ni(S$_4$)}$_2$$Fe_4S_4I_2$] (**4**) two neutral Ni complexes serve as terminal ligands for two iron atoms of an Fe_4S_4 cubane cluster *via* μ_2-bridging thiolate functions of the EtN_2S_2 and S_4 ligands, respectively. The μ_2-S(thiolate)-bridged clusters crystallize from the reaction mixtures and can be easily isolated in almost quantitative yield. The monosubstituted cluster [{Ni(EtN_2S_2)}-$Fe_4S_4I_3$]$^-$ (for the crystal structure see ref 27), in which only one Ni complex is attached to an Fe_4S_4 unit, has also been obtained, but so far only as a "salt" of the trinuclear counterion [{Ni(EtN_2S_2)}$_2$Ni]$^{2+}$.[33]

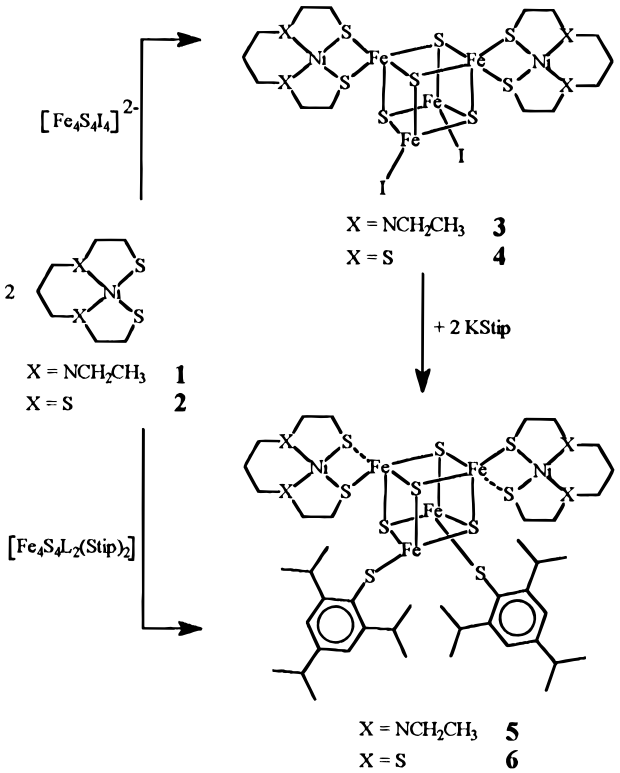

Figure 2. Synthesis of the μ_2-SR-bridged assemblies **3**−**6**. The same structural representations have been chosen for **3** and **4**, though no structural details are available for **4**. Reactions leading to **4** and **6** were performed in dichloromethane solution. **3** and **5** were synthesized in acetonitrile solution.

The substitution reactions leading to **3** and **4** are rare examples for the displacement of an anionic ligand of an Fe_4S_4 core by a neutral molecule. This behavior has been observed so far only for a few other uncharged ligands. For example, 1,4,7-triazacyclononane and 1,2-bis-(dimethylphosphino)ethane are able to displace halogens from [Fe_4S_4(LS_3)X]$^{2-}$,[34,35] whereas *tert*-butyl isocyanide can displace halogens or thiolates from [$Fe_4S_4X_4$]$^{2-}$.[36]

(33) The directed synthesis of this cluster anion was achieved, using acetonitrile as solvent and stoichiometric amounts of [$Fe_4S_4I_4$]$^{2-}$, **1**, and Ni(ClO_4)$_2$·6CH_3CN to generate the [{Ni(EtN_2S_2)}$_2$Ni]$^{2+}$ cation *in situ*. However, due to the low solubility of the salt in common organic solvents (the monosubstituted cluster is slightly soluble in 1,2-propylene carbonate and 1,3-dimethylimidazolidin-2-one) and the fact that charged Fe_4S_4 clusters with unsymmetrical substitution pattern are prone to disproportionation in solution,[34] the characterization of this $NiFe_4S_4$ cluster was not further developed.

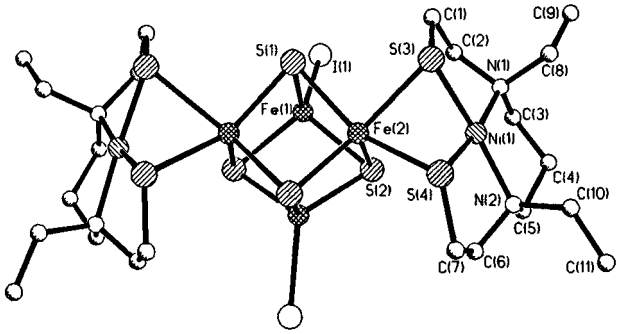

Figure 3. Crystal structure of $[\{Ni(EtN_2S_2)\}_2Fe_4S_4I_2]$ (**3**) with the atom labeling scheme. Hydrogen atoms are omitted. **3** exhibits crystallographic C_2 symmetry.

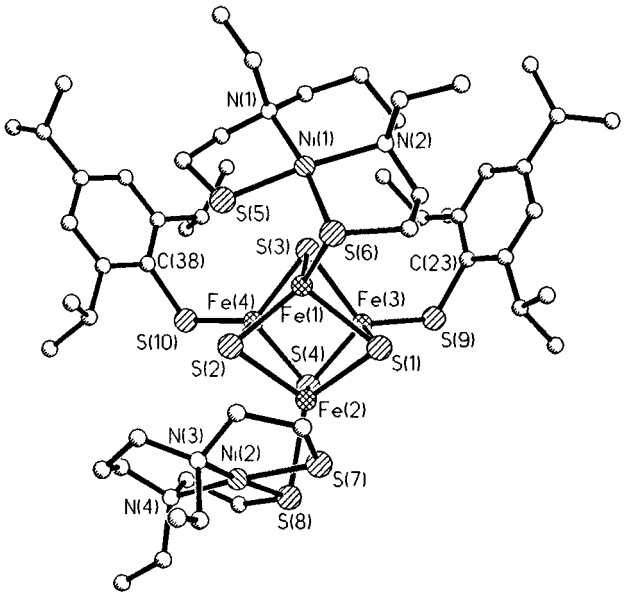

Figure 4. Crystal structure of $[\{Ni(EtN_2S_2)\}_2Fe_4S_4(Stip)_2]$ (**5**) with the atom labeling scheme for selected atoms. Hydrogen atoms have been omitted.

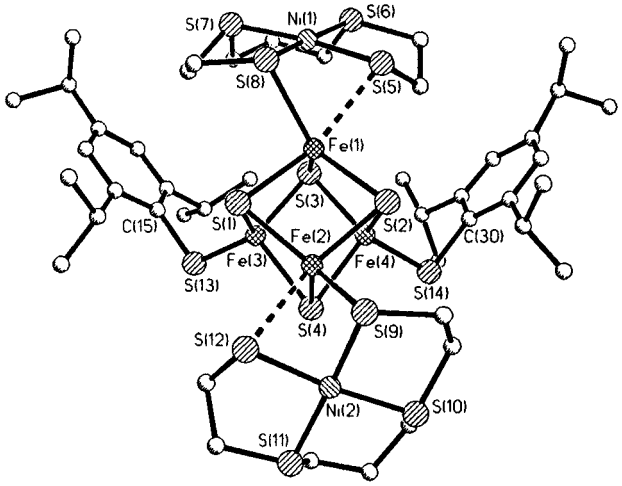

Figure 5. Crystal structure of $[\{Ni(S_4)\}_2Fe_4S_4(Stip)_2]$ (**6**) with the atom labeling scheme for selected atoms. Hydrogen atoms have been omitted.

Table 2. Selected Interatomic Distances (pm) and Angles (deg) for $[\{Ni(EtN_2S_2)\}_2Fe_4S_4I_2]$ (**3**)

Ni Coordination			
Ni(1)−N(2)	198.2(6)	N(1)−Ni(1)−S(3)	88.2(2)
Ni(1)−N(1)	200.0(7)	N(2)−Ni(1)−S(4)	88.7(2)
Ni(1)−S(3)	215.8(2)	S(3)−Ni(1)−S(4)	82.00(9)
Ni(1)−S(4)	217.8(2)	N(2)−Ni(1)−N(1)	101.1(3)
Ni(1)···S(2)	317.6(2)	Σ	360.0
Bridging Units			
Ni(1)−Fe(2)	282.7(2)	Ni(1)−S(4)−Fe(2)	73.32(7)
Fe(2)−S(4)	253.3(2)	Ni(1)−S(3)−Fe(2)	75.08(7)
Fe(2)−S(3)	246.4(2)	S(3)−Fe(2)−S(4)	69.39(7)
Fe_4S_4 Core			
Fe(1)−Fe(2)	278.4(2)	Fe(1)−S(1)	221.9(2)
Fe(1)−Fe(2′)	278.2(2)	Fe(1)−S(2)	230.0(2)
Fe(1)−Fe(1′)	280.4(2)	Fe(1′)−S(2)	229.0(2)
Fe(2)−Fe(2′)	311.3(2)	Fe(2)−S(1)	235.6(2)
mean of 6	284.2	Fe(2)−S(1′)	230.9(2)
		Fe(2)−S(2)	228.2(2)
Fe(1)−I(1)	256.4(1)	mean of 6	229.3

On both **3** and **4** the iodide ligands can be replaced by thiolates by a metathesis reaction with solid potassium 2,4,6-triisopropylbenzenethiolate (KStip), to give $[\{Ni(EtN_2S_2)\}_2Fe_4S_4(Stip)_2]$ (**5**) and $[\{Ni(S_4)\}_2Fe_4S_4(Stip)_2]$ (**6**) in moderate yields (88% and 52%, respectively). This ligand substitution reaction can also be extended to alkanethiolates, *e.g.*, ethane- or 2-methylpropane-2-thiolate, but afford the thiolate-bound clusters generally in lower yields. Alternatively, **5** and **6** can be synthesized in a one-step procedure by reaction of the Ni complexes with the neutral cluster $[Fe_4S_4(Stip)_2(tap)_2]$ (tap = thioantipyrine = 2,3-dimethyl-1-phenyl-3-pyrazoline-5-thione)[29] in acetonitrile. In this reaction the Ni complexes **1** and **2** displace neutral sulfur-bound thioantipyrine at two iron sites of an Fe_4S_4 cubane cluster. Since no neutral alkanethiolate clusters of the type $[Fe_4S_4(SR)_2L_2]$ are known, this route is limited to synthesis of arenethiolate-substituted $Ni_2Fe_4S_4$ clusters.

Description of the Structures. **3**, **5**, and **6** (see Figures 3−5) form isolated neutral species in the solid state. Crystal data are summarized in Table 1, and selected interatomic distances and angles are collected in Tables 2−4.

The mononuclear neutral Ni(II) complexes with 4-fold planar N_2S_2 (**3**, **5**) or S_4 (**6**) coordination of the metal ion are attached to an iron−sulfur cluster *via* bridging thiolates in each compound. Ligation of the $[Fe_4S_4]^{2+}$ core is completed by two iodide (**3**) and two thiolate (**5**, **6**) anions. However, there are significant differences between the Ni−Fe bridging modes, which also affect the geometry of the Fe_4S_4 clusters. The gradual change of this Ni−Fe bridging by thiolate from **3** over **6** to **5**, *i.e.*, from bidentate to monodentate, is the most interesting feature of these structures. Therefore, a direct comparison of the three structures is the obvious choice.

Structure of the Bridging Units. The crystallographic C_2 symmetry of **3** leads to two identical fragments with nearly symmetric bidentate thiolate coordination at two of the four Fe cluster atoms. The Fe(2)−S(3) and Fe(2)−S(4) distances were found to be 246.4(2) and 253.3(2) pm, respectively. This, together with the folded structure of the resulting four-membered NiS_2Fe ring,[37] results in a Ni−Fe distance of 282.7(2) pm, which is considerably shorter than the Fe(2)−Fe(2′) distance within the Fe−S cluster (311.3(2) pm).

In **6** an unsymmetric coordination of the two $[Ni(S_4)]$ units to the Fe_4S_4 cluster is observed. The resulting Fe−S distances are 246.0(3) and 266.2(4) pm at Fe(1) and 243.4(3) and 274.9(4) pm at Fe(2). Consequently, the Ni−Fe distances (Ni(1)−Fe(1) = 298.9(2) pm and Ni(2)−Fe(2) = 296.7(2) pm) are longer than in **3** and the corresponding Fe−Fe distance is shorter (Fe(1)−Fe(2) = 299.8(2) pm).

(34) Holm, R. H.; Ciurli, S.; Weigel, J. A. *Prog. Inorg. Chem.* **1990**, *38*, 1 and literature cited therein.

(35) Holm, R. H. *Adv. Inorg. Chem.* **1992**, *38*, 1 and literature cited therein.

(36) Goh, C.; Weigel, J. A.; Holm, R. H. *Inorg. Chem.* **1994**, *33*, 4861.

(37) The folded structure of the Ni−S−Fe bridges in **3**, **6**, and **5** is a result of the binding geometry of the bridging thiolate S atoms and can be observed in other compounds, too, in which derivatives of $[Ni(EtN_2S_2)]$ bind to mononuclear transition metals.[17−19,21,22,25,26]

Table 3. Selected Interatomic Distances (pm) and Angles (deg) for $[\{Ni(EtN_2S_2)\}_2Fe_4S_4(Stip)_2]$ (**5**)

Ni Coordination			
Ni(1)−N(1)	200(2)	Ni(2)−N(3)	197.8(14)
Ni(1)−N(2)	201.9(14)	Ni(2)−N(4)	201.0(14)
Ni(1)−S(5)	215.5(5)	Ni(2)−S(7)	215.0(5)
Ni(1)−S(6)	218.2(5)	Ni(2)−S(8)	217.8(5)
Ni(1)···S(3)	337.8	Ni(2)···S(2)	328.1
N(1)−Ni(1)−N(2)	99.6(6)	N(3)−Ni(2)−N(4)	99.4(6)
N(1)−Ni(1)−S(5)	88.8(5)	N(3)−Ni(2)−S(7)	88.9(5)
N(2)−Ni(1)−S(6)	88.8(4)	N(4)−Ni(2)−S(8)	89.1(4)
S(5)−Ni(1)−S(6)	82.7(2)	S(7)−Ni(2)−S(8)	82.6(2)
Σ	359.9	Σ	360.0
Bridging Units			
Ni(1)−Fe(1)	291.4(3)	Ni(2)−Fe(2)	289.4(3)
Fe(1)−S(6)	236.1(5)	Fe(2)−S(8)	242.6(5)
Fe(1)···S(5)	294.1(5)	Fe(2)···S(7)	281.2(5)
Ni(1)−S(6)−Fe(1)	79.7(2)	Ni(2)−S(8)−Fe(2)	77.7(2)
Fe_4S_4 Core			
Fe(1)−Fe(2)	284.0(3)	Fe(1)−S(1)	239.8(5)
Fe(1)−Fe(3)	287.2(3)	Fe(1)−S(2)	226.6(5)
Fe(1)−Fe(4)	274.2(3)	Fe(1)−S(3)	232.8(4)
Fe(2)−Fe(3)	281.7(3)	Fe(2)−S(1)	226.0(5)
Fe(2)−Fe(4)	285.0(3)	Fe(2)−S(2)	231.4(5)
Fe(3)−Fe(4)	275.5(3)	Fe(2)−S(4)	239.9(5)
mean of 6	281.3	Fe(3)−S(1)	227.5(5)
		Fe(3)−S(3)	230.8(4)
Fe(3)−S(9)	227.5(4)	Fe(3)−S(4)	223.6(5)
Fe(4)−S(10)	226.5(5)	Fe(4)−S(2)	230.1(4)
		Fe(4)−S(3)	225.8(5)
		Fe(4)−S(4)	229.3(4)
		mean of 12	230.3

Table 4. Selected Interatomic Distances (pm) and Angles (deg) for $[\{Ni(S_4)\}_2Fe_4S_4(Stip)_2]$ (**6**)

Ni Coordination			
Ni(1)−S(5)	216.2(3)	Ni(2)−S(9)	216.2(3)
Ni(1)−S(6)	216.2(3)	Ni(2)−S(10)	217.6(4)
Ni(1)−S(7)	217.8(3)	Ni(2)−S(11)	217.2(4)
Ni(1)−S(8)	217.1(3)	Ni(2)−S(12)	216.4(4)
Ni(1)···S(3)	344.3	Ni(2)···S(4)	339.5
S(5)−Ni(1)−S(8)	84.6(1)	S(9)−Ni(2)−S(12)	84.5(1)
S(6)−Ni(1)−S(5)	90.5(1)	S(12)−Ni(2)−S(11)	91.5(2)
S(6)−Ni(1)−S(7)	95.1(1)	S(11)−Ni(2)−S(10)	93.2(2)
S(8)−Ni(1)−S(7)	89.9(1)	S(9)−Ni(2)−S(10)	91.6(2)
Σ	360.1	Σ	360.8
Bridging Units			
Ni(1)−Fe(1)	298.9(2)	Ni(2)−Fe(2)	296.7(2)
Fe(1)−S(8)	246.0(3)	Fe(2)−S(9)	243.4(3)
Fe(1)···S(5)	266.2(4)	Fe(2)···S(12)	274.9(4)
Ni(1)−S(5)−Fe(1)	75.8(1)	Ni(2)−S(9)−Fe(2)	80.2(1)
Ni(1)−S(8)−Fe(1)	80.1(1)	Ni(2)−S(12)−Fe(2)	73.2(1)
S(5)−Fe(1)−S(8)	69.3(1)	S(9)−Fe(2)−S(12)	68.0(1)
Fe_4S_4 Core			
Fe(1)−Fe(4)	278.5(2)	Fe(1)−S(1)	239.1(3)
Fe(1)−Fe(3)	284.6(2)	Fe(1)−S(2)	229.2(3)
Fe(1)−Fe(2)	299.8(2)	Fe(1)−S(3)	228.0(3)
Fe(2)−Fe(3)	280.2(2)	Fe(2)−S(1)	230.5(3)
Fe(2)−Fe(4)	282.1(2)	Fe(2)−S(2)	236.6(3)
Fe(3)−Fe(4)	275.4(2)	Fe(2)−S(4)	227.7(3)
mean of 6	283.4	Fe(3)−S(1)	226.0(3)
		Fe(3)−S(3)	230.2(3)
Fe(4)−S(14)	226.7(3)	Fe(3)−S(4)	230.0(3)
Fe(3)−S(13)	228.0(3)	Fe(4)−S(2)	223.6(3)
		Fe(4)−S(3)	229.8(3)
		Fe(4)−S(4)	230.4(3)
		mean of 12	230.1

In **5** the two neutral amino thiolate−nickel(II) complexes act as essentially monodentate ligands. The Fe−S distances to the bridging thiolates are 236.1(5) pm for Fe(1)−S(6) and 242.6(5) pm for Fe(2)−S(8). However, the interactions with the second thiolate, Fe(1)−S(5) (294.1(5) pm) and especially Fe(2)−S(7) (281.2(5) pm), may be regarded as weak "secondary" bonds. Though the Ni−Fe distances (291.4(3) and 289.4(3) pm) are shorter than in **6**, a Fe(1)−Fe(2) distance is observed, which again is shorter; it was found to be 284.0(3) pm.

Table 5. Electrochemical Data.

	reduction	1st oxidation	2nd oxidation
3	−750[a]	+160[b] (80; 0.92)	+720
3b[51]	−790	+140 (60; 0.94)	+680[c] (62; 0.77)
5	−1050 (100; 0.65)	+0 (90; 0.79)	+485 (145; 0.59)
6	−970	+110, +210	+610

[a] Value given as E_p (mV) *vs* SCE. [b] Value given as $E_{1/2}$ (mV) (ΔE_p (mV); I_{pa}/I_{pc}) *vs* SCE with I_{pa}/I_{pc} corrected according to Nicholson et al.[52] [c] At 400 mV/s.

Ni Coordination. The distances and angles within the nickel complex fragments of **3** and **5** are almost identical and very similar to those observed in $[Ni(MeN_2S_2)]$, in which the N atoms are methylated.[16] In **3** the S(3)−Ni(1)−S(4) angle of 82.00(9)° is smaller by 3° whereas the N(1)−Ni(1)−N(2) angle of 101.1(3)° is larger by 4° compared to those in the mononuclear compound.

The $[Ni(S_4)]$ fragments in **6** exhibit similar distortions when compared to the mononuclear complex **2**.[14] Here the decrease of the S−Ni−S angles is accompanied by a slight tetrahedral distortion of the S_4 plane, which is more pronounced for the Ni(2)-containing fragment.[38]

It should be noted that for all bridged assemblies relative short distances between a Ni ion and a sulfide of the Fe_4S_4 cluster can be observed, which are a result of the folded geometry of Ni complexes and Fe_4S_4 fragments. These distances (between 317.6 pm for **3** and 344.3 pm for **6**) must be termed as still nonbonding but might become bonding, if the folding around the bridging thiolate S atoms would be more pronounced. For **5** and **6** the longer $Ni-S_{sulfide}$ distances are possibly a result of the bulky thiolates which prevent close contacts between the Ni^{2+} ions and the sulfur atoms of the Fe/S cluster.

Fe_4S_4 Geometry. The Fe_4S_4 cores in **3**, **5**, and **6** exhibit distortions (see Tables 3−5), which significantly differ from those commonly observed for symmetrically substituted $[Fe_4S_4X_4]^{2-}$ clusters (X = Hal, SR).[30,39] Moreover, the average Fe−Fe distances, not the average Fe−S distances, of the thiolate-bridged assemblies (see Tables 2−4) are considerably longer than those of $[Fe_4S_4X_4]^{2-}$ cluster anions (Fe−Fe, between 272.9 and 276.6 pm; Fe−S, between 225.7 and 229.4 pm; X = Cl, I, SR).[39,40] Both distortions of the Fe_4S_4 cores and elongation of the Fe−Fe distances are a result of the different coordination geometries of the Fe atoms incorporated in the bridging units and of their coordination numbers (4- or 5-fold coordination). This unequivocally follows from comparison of the structures of the Fe_4S_4 cores in **3** and **6** with that of the $[Fe_4S_4(dtc)_2X_2]^{2-}$ anion (dtc = *N*,*N*-diethyldithiocarbamate; X = Cl^-, PhS^-), which exhibits similar distortions.[41]

Discussion. According to a mechanistic proposal for acetyl-CoA formation at center A of Ni−CO dehydrogenase, both Fe

(38) S(5) and S(7) deviate by +6 and +5.4 pm and S(6) and S(8) by −5.4 and −6.0 pm, respectively, from the least-squares plane of these four atoms, whereas S(10,12) are located 13.2 pm above and S(9,11) are located 12.1 pm below the least-squares plane of the Ni-coordinated S atoms.

(39) Pohl, S.; Saak, W. *Z. Naturforsch.* **1988**, *43b*, 457 and literature cited therein.

(40) Mascharak, P. K.; Hagen, K. S.; Spence, J. T.; Holm, R. H. *Inorg. Chim. Acta* **1983**, *80*, 157.

(41) In $[Fe_4S_4(dtc)_2X_2]^{2-}$ two five-coordinated Fe atoms bind two bidentate diethyldithiocarbamate (dtc) ligands and two four-coordinated Fe atoms bind either chloride or benzenethiolate. The Fe−Fe distances between the five-coordinated Fe atoms (304.5(4) pm for X = Cl^- and 305.3 (3) pm for X = PhS^-) are considerably long, and the Fe_4S_4 core exhibits distortions, which are similar to those of **3** and **6**. (a) Kanatzidis, M. G.; Coucouvanis, D.; Simopoulos, A.; Kostikas, A.; Papaefthymiou, V. *J. Am. Chem. Soc.* **1985**, *107*, 4925. (b) Kanatzidis, M. G.; Ryan, M.; Coucouvanis, D.; Simopoulos, A.; Kostikas, A. *Inorg. Chem.* **1983**, *22*, 179.

and Ni of the Ni−Y−Fe_4S_4 cluster serve as binding sites for CO and a CH_3 group, respectively. The crystal structures of **3**, **5**, and **6**, which reveal open sites at the μ_2-S-bound five- or four-coordinated Fe atoms and at the square planar coordinated Ni ions, are consistent with the concept of substrate binding at these centers.

Another important result of the crystallographic studies is that variations in the Ni donor set and in the character of terminal ligands of the Fe_4S_4 core can substantially change not only the structure but also the constitution of the bridged assemblies. The binding of substrate molecules at the Ni and Fe centers or a change in oxidation level of the Ni−Y−Fe_4S_4 assembly could possibly effect similar structural variations in the active sites of Ni−CODH/ACS, which might be essential to the catalytic properties of the enzyme.

The origin of the structural differences should be seen in the deviating electronic properties, not in the steric demands, of the individual terminal ligands of the Fe atoms (iodide in **3**, thiolate in **5**) and of the coordination environment of the Ni ions (N_2S_2 in **5**, S_4 in **6**). This is clearly illustrated by the crystal structure of the closely related cluster [{Ni(*n*-BuN_2S_2)}$_2$$Fe_4S_4$-$(SMe)_2$], in which the bulky 2,4,6-triisopropylbenzene groups have been replaced by small methyl groups. As in **5**, a monodentate ligation of the [Ni(*n*-BuN_2S_2)] complexes is observed (Fe−$S_{bridging}$ = 242.1(4) and 283.0 pm; Ni−Fe = 296.9(2) pm) and the Fe−Fe distance between the μ_2-S-ligated iron atoms is shortened to 280.7(4) pm. Investigations on this methanethiolate-ligated cluster have not been included in this work since it could not be isolated in pure form.[42]

As opposed to the structure of the bridging units and the Fe_4S_4 clusters, the coordination geometries of the Ni ions in the bridged assemblies are very similar to each other and resemble those of the mononuclear complexes. They are in good agreement with the Ni EXAFS results that were obtained for the enzymes: The α subunit of the enzyme from *C. thermoaceticum*, which is believed to contain center A, exhibits EXAFS properties consistent with a Ni center located in a distorted square planar coordination sphere of two S and two N/O donors with metal−ligand distances of 219 and 189 pm, respectively,[9] whereas the Ni environment of center C, as studied on the enzyme from *R. rubrum*, is proposed to be distorted tetrahedral or five-coordinate with 2 S atoms at 223 pm and 2−3 N/(O) atoms at 187 pm.[8] The average Ni−μ_2-S distances of 216.8 pm in **3** and 216.6 pm in **5** agree with the EXAFS results. However, the average Ni−N distances of 199.1 pm in **3** and 200.2 pm in **5** are considerably longer than those in the enzyme. As square planar Ni complexes with primary amines exhibit smaller Ni−N distances, this seems to be a consequence of the bulky tertiary amino functions of the EtN_2S_2 ligand.[43]

As has been noted above, pentacoordination of the Ni ions in the bridged assemblies could be achieved by a more bent conformation of the Ni complex fragments which would allow an additional Ni−S contact between one sulfide atom of the Fe_4S_4 core and the Ni ion. The resultant five-coordination of the Ni atom, which has been proposed by Cramer et al. for the Ni atom in center A of *C. thermoaceticum*,[44] would also change the electronic ground state of the square pyramidal Ni(II) and hence its affinity for binding of one additional donor molecule (substrate) in an axial position.

^{1}H-NMR Spectra. ^{1}H-NMR spectra of the bridged assemblies **3, 5,** and **6** together with the spectrum of the mononuclear complex **1** are shown in Figure 6.

The NMR spectra of the clusters display isotropically shifted signals for the Fe_4S_4-bound Ni complexes, which result from the excitation of electrons into paramagnetic states of the $[Fe_4S_4]^{2+}$ core. The shift mechanism is believed to be mainly contact in origin.[45] Though some of the resonances of the EtN_2S_2 or S_4 ligands could not be assigned unambiguously, the spectra prove that the heterometallic clusters retain their bridged structures in solution.

[{Ni(EtN_2S_2)}$_2$$Fe_4S_4I_2$] (3). For **3** the most downfield shifted signals (i)/(j) appear at a value typical of protons of thiolate ligands in tetraalkanethiolate-substituted $[Fe_4S_4(SR)_4]^{2-}$ clusters[46] and thus seem to correspond to the thiolate-bound methylene groups. The integral intensities for (i)/(j) are consistent with eight protons per formula. This demonstrates that in solution the Ni-containing fragments are bound to the Fe_4S_4 core *via* two bridging S (thiolate) functions, which is in agreement with the crystal structure of **3**. Remarkably, two peaks for axial and equatorial protons indicate chemical inequivalence of the protons (i)/(j), whereas in the spectrum for the monomeric complex (**1**) only one resonance for these protons at 2.56 ppm is found. Apparently, on the NMR time scale no inversion of conformation of the μ_2-S-(thiolate) functions occurs, which would lead to chemical equivalence of these diastereotopic protons. A similar behavior was found in the NMR spectra of protein-bound Fe_4S_4 clusters, in which two or more signals for the β-CH_2 groups of the geometrically fixed cysteinethiolate residues are observed.[46−48]

[{Ni(EtN_2S_2)}$_2$$Fe_4S_4$(Stip)$_2$] (5). Due to the change in ligation of the Fe_4S_4 core, the extent of the downfield shift for the protons (m)/(l) of the S-bound methylene groups is decreased and the signals of these protons move to 15.26 and 12.76 ppm, respectively. Since the integral intensities of signals (l)/(m) are consistent with eight protons per formula, the Fe_4S_4 core in **5** seems to be coordinated symmetrically by four μ_2-bridging thiolates of two EtN_2S_2 ligands, which would be in contrast to the structure in the solid state where each metallothiolate acts as a monodentate ligand. The interpretation of bidentate binding in solution is supported by the low number of resonances for the symmetry-equivalent protons of the EtN_2S_2 ligands (mirror symmetry) and by the relative arrangement of the resonances, which resembles that of **3**. Alternatively, the spectrum of **5** might be interpreted in terms of monodentate binding of each Ni complex, if one assumes a fluxional exchange of the identity of bridging and nonbridging thiolate S atoms. On average, two Fe atoms of the Fe_4S_4 cluster would then be four-coordinated, in agreement with the crystal structure of the compound.

(42) The cluster [{Ni(*n*-BuN_2S_2)}$_2$$Fe_4S_4$$(SCH_3)_2$], which contains *n*-butyl instead of ethyl groups at the nitrogen atoms, is available by a reaction sequence similar to that outlined for **3b** in ref 51 (starting from *n*-butyric chloride and 1,3-diaminopropane), followed by metathesis with potassium methanethiolate in THF. Black crystals of the thiolato cluster suitable for single X-ray crystallography were grown from CH_2Cl_2/THF solution but were found to be contaminated with isomorphous [{Ni(*n*-BuN_2S_2)}$_2$$Fe_4S_4$-$Cl_2$], a decomposition product from the reaction with dichloromethane. Both compounds crystallize in the monoclinic space group *C*2/*c* as a solvate with one molecule of CH_2Cl_2. a = 1958.0(3) pm, b = 2266.2(4) pm, c = 1586.4-(2) pm, β = 126.71(1)°, and Z = 4. The structure was refined to R_1 = 0.0849 (wR_2 = 0.1863) with occupancy factors of 0.5 for each SCH_3 and Cl.

(43) In the trinuclear complex [Ni{Ni($H_2NCH_2CH_2S)_2$}$_2$]$^{2+}$ Ni−N distances of 190.2(7) and 192.6(7) pm were found[22] that are equal to those of *trans*-[bis(L-cysteinato-*N*,*S*)nickelate(II)].[23]

(44) Cramer, S. P.; Eidsness, M. K.; Pan, W.-H.; Morton, T. A.; Ragsdale, S. W.; DerVartanian, D. V.; Ljungdahl, L. G.; Scott, R. A. *Inorg. Chem.* **1987**, *26*, 2477.

(45) The isotropic shifts of the protons of the arene groups in **5**, referenced to the corresponding disulfide ($CDCl_3$), are +1.30 ppm (Ar-H), +1.77 ppm (*o*-CH), +0.53 ppm (*p*-CH), +0.66 ppm (*o*-CH_3), and −0.08 (*p*-CH_3). These values compare well with those of other arenethiolate-substituted Fe_4S_4 clusters for which a contact shift mechanism is dominant. See: Weigel, J. A.; Holm, R. H. *J. Am. Chem. Soc.* **1991**, *113*, 4184.

(46) Holm, R. H.; Phillips, W. D.; Averill, B. A.; Mayerle, J. J.; Herskovitz, T. *J. Am. Chem. Soc.* **1974**, *96*, 2109.

(47) Barclay, J. E.; Evans, D. J. *Inorg. Chim. Acta* **1996**, *247*, 113.

(48) Reynolds, J. G., Laskowski, E. J., Holm, R. H. *J. Am. Chem. Soc.* **1978**, *100*, 5315.

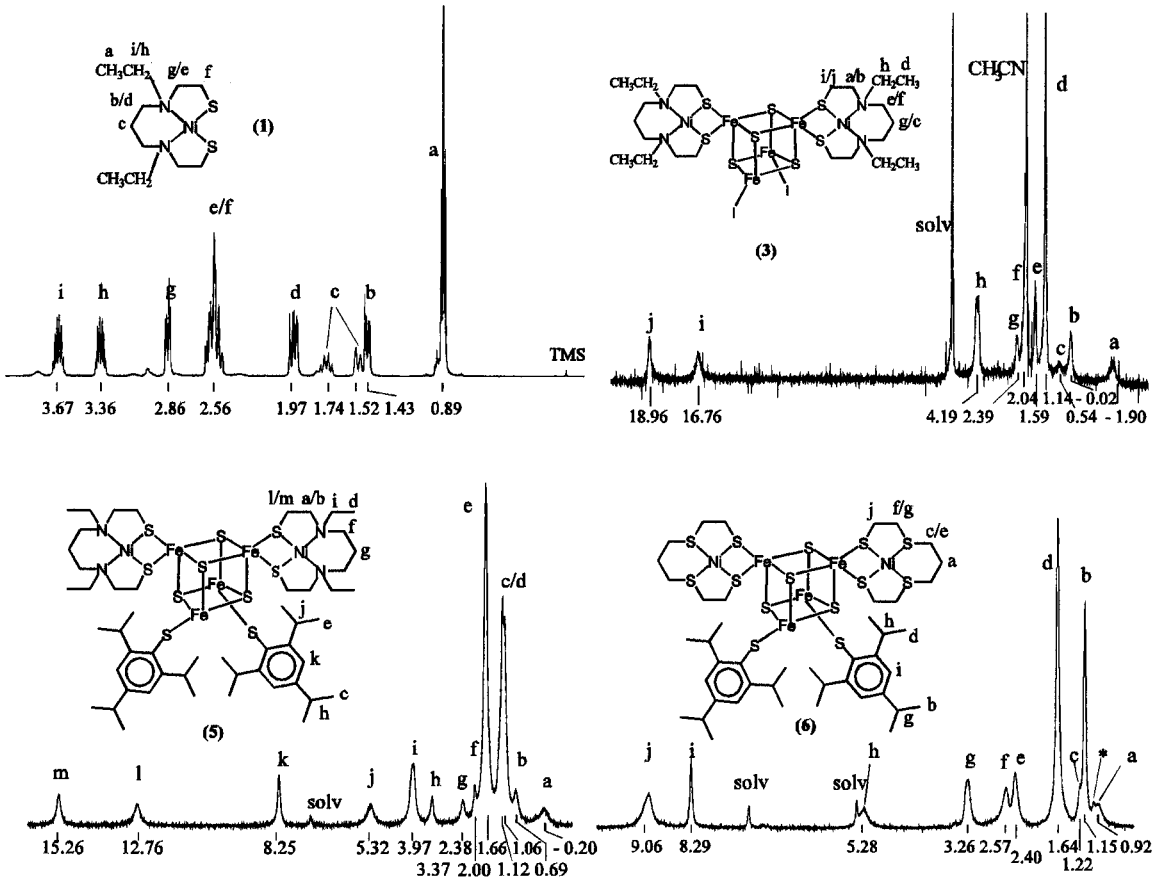

Figure 6. ^{1}H-NMR spectra of **1** in CD_3CN (500 MHz), **3** in CD_2Cl_2 (300 MHz), **5** in $CDCl_3$ (500 MHz), and **6** in $CD_2Cl_2/CDCl_3$ (300 MHz). All spectra were recorded at 297 K. Signal positions [ppm] were referenced against TMS or against the signals of the solvents (solv). **1**: The protons labeled as (g)/(e), (i)/(h), and (b)/(d) are diasterotopic because of the fixed configuration of the Ni-bound N atoms. Due to hindered rotation and ^{1}H−^{1}H coupling the protons (c) appear as multiplets, too. The protons of the thiolate-bound methylene groups (f), due to the coupling with protons (g)/(e), give a broad pseudosinglet whereas the protons of the methyl groups (a) appear as a triplet. **3**: Signal (f) is obscured by the crystal solvent acetonitrile. (a)/(b), (e)/(f), and (g)/(c) were tentatively assigned on the basis of signal intensity and signal shape. **5**: The assignment of resonances is tentative for (a)/(b), (f), and (g). **6**: The signals (a)/(c), (e)/(f), and (g) could not be assigned unambiguously. An asterisk designates an impurity.

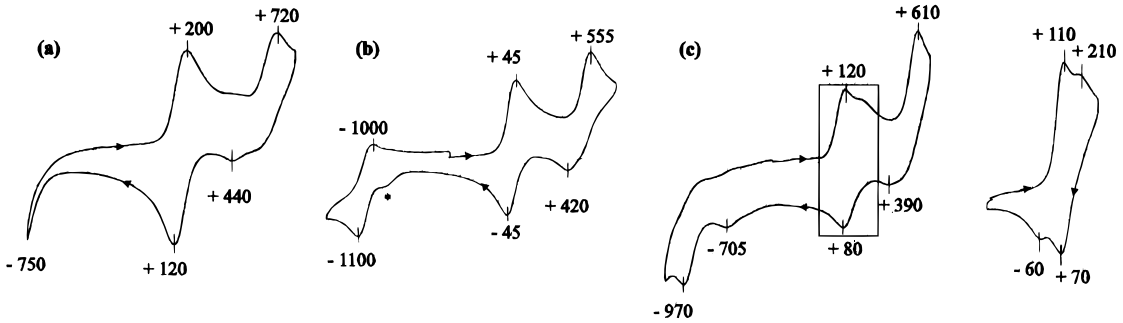

Figure 7. Cyclic voltammograms of $[\{Ni(EtN_2S_2)\}_2Fe_4S_4I_2]$ (**3**) (a), $[\{Ni(EtN_2S_2)\}_2Fe_4S_4(Stip)_2]$ (**5**) (b), and $[\{Ni(S_4)\}_2Fe_4S_4(Stip)_2]$ (**6**) (c) in CH_2Cl_2 solutions. For **6** a second cyclic voltammogram is shown, which was recorded independently within the boundaries indicated by the frame. Potentials (mV) were referenced against SCE. (b) An asterisk designates a decomposition product from the oxidation process at +555 mV.

$[\{Ni(S_4)\}_2Fe_4S_4(Stip)_2]$ (6). In the ^{1}H-NMR spectrum of **6** axial and equatorial protons of the μ_2-SCH_2R groups occur as one signal at 9.06 ppm. Since in the spectrum of the related compound $[\{Ni(S_4)\}_2Fe_4S_4(Sdur)_2]$ (not shown, SDur = 2,3,5,6-tetramethylbenzenethiolate) two μ_2-SCH_2R resonances at 9.55 and 10.35 ppm were observed, the overlapping of the corresponding signals in **6** seems to be coincidental. Compared to the ethylamino derivatives **3** and **5**, the downfield shifts are less distinct for **6**. Obviously, the unpaired spin density delocalized from the Fe_4S_4 cluster to protons of the ligand is lower than in **5**. This behavior correlates with the weaker binding of the Ni complexes with the S_4 donor set to iron atoms of the Fe_4S_4 cluster, which is also demonstrated by long Fe−Ni distances in the crystal structure of this compound. The μ_2-bridging thiolates appear to bind symmetrically to the Fe_4S_4 core, as follows from the integral intensity of the signals for the protons labeled as (j), and from the low number of resonances of the remaining symmetrically equivalent protons of the S_4 ligand, whose tentative assignment is outlined in Figure 6. As mentioned for **5**, a rapid transposition of two unsymmetrically bound $[Ni(S_4)]$ fragments might be an alternative interpretation.

Electrochemical Properties. Cyclic voltammograms of $[\{Ni(EtN_2S_2)\}_2Fe_4S_4I_2]$ (**3**) (a), $[\{Ni(EtN_2S_2)\}_2Fe_4S_4(Stip)_2]$ (**5**) (b), and $[\{Ni(S_4)\}_2Fe_4S_4(Stip)_2]$ (**6**) (c) recorded in CH_2Cl_2 solutions with 0.1 M (n-Bu_4N)PF_6 as supporting electrolyte are shown in Figure 7. The scan rate was 100 mV/s. The electrochemical data are summarized in Table 5.

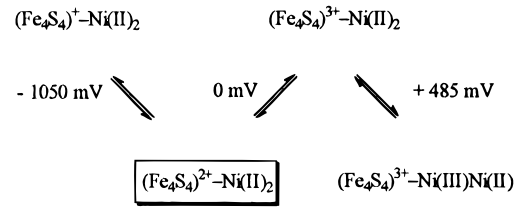

Figure 8. Tentative assignment of the different redox states of **5**.

3 may be consecutively oxidized at +160 and +720 mV (*vs* SCE) and reduced at −750 mV. Only the oxidation process at +160 mV is quasi-reversible. The reduction peak at +440 mV corresponds to an unidentified species that is generated electrochemically at +720 mV. Upon substitution of terminal iodides by thiolate, all redox processes shift toward lower values and become quasi-reversible. For **5** oxidations occur at 0 and +485 mV; a reduction process is observed at −1050 mV.

6 exhibits a more complex redox behavior. The compound is reduced irreversibly at −970 mV and oxidized irreversibly at +610 mV. During the oxidation a small amount of a compound forms that can be reduced at −705 mV. In contrast to **3** and **5** the oxidation wave at +120 mV seems not to reflect a one-electron oxidation process, because when viewed independently from the other redox events (see the right cyclic voltammogram in Figure 7c), both the oxidation and the reduction waves split into two waves. Theses waves possibly correspond to two subsequent one-electron oxidation processes.

At least for **3** and **5** the observed redox processes are believed to refer to equal redox states. On the basis of the assumption that all observed quasi-reversible redox processes are one-electron processes,[49] the different redox states for **5** were tentatively assigned as shown in Figure 8. According to this scheme, the reduction at −1050 mV is believed to be centered primarily on the Fe_4S_4 core, as was concluded from the dependence of both the wave value and its degree of reversibility on the nature of Fe_4S_4-bound terminal ligands, iodide, or thiolate. Moreover, tetrathiolate-bound $[Fe_4S_4(SR)_4]^{2-}$ clusters are reduced at similar potentials in DMF solution (−830 to −1480 mV *vs* SCE).[40]

However, one-electron reduction of one Ni(II) center cannot be ruled out. Darensbourg et al.[21] reported electrochemical generation of a Ni(I) species from a mononuclear Ni(II)-amino thiolate complex in acetonitrile solution at −2180 mV (SCE). The reduction potential shifted toward more positive potentials when the Ni(II) complex was part of an oligonuclear structure with μ_2-bridging thiolates.

The potential for the first oxidation process of **5** is highly dependent on the identity of the terminal ligands at the Fe_4S_4 core, *e.g.*, iodide in **3** (+160 mV) and thiolate in **5** (0 mV) and in addition fits between those observed for the redox couples $[Fe_4S_4I_4]^{1-/2-}$ (+435 mV in CH_2Cl_2) and $[Fe_4S_4(S\text{-}tBu)_4]^{1-/2-}$ (−110 mV in DMSO),[50] which suggests an $[Fe_4S_4]^{2+/3+}$ oxidation process. The second oxidation process at +485 mV seems to reflect a Ni(II)-centered reaction. This process is irreversible for **3**, but quasi-reversible for $[\{Ni(BenzN_2S_2)\}_2\text{-}Fe_4S_4I_2]$ (not shown; **3b** in Table 5) which contains benzyl instead of ethyl groups at the N atoms.[51] The interpretation of this redox process in terms of a Ni(II)/(III) oxidation is supported by the fact that no Fe_4S_4 cluster is known to our knowledge that is stable in the $[Fe_4S_4]^{4+}$ state and thus consists entirely of Fe(III) ions.

Summary

(i) The Ni complexes **1** and **2**, which contain Ni(II) in square planar N_2S_2 and S_4 environments, respectively, react with $[Fe_4S_4I_4]^{2-}$ to give the clusters **3** and **4** in almost quantitative yields. In the resultant compounds two Ni complexes are covalently bound to an Fe_4S_4 core *via* μ_2-bridging thiolates of the metallo ligands. The Ni coordination geometry of the [Ni(EtN_2S_2)] complex remains nearly unchanged upon binding to the Fe_4S_4 unit.

(ii) In **3** and **4** the iodide ligands of the Fe_4S_4 cubane can be displaced by arenethiolates, yielding **5** and **6**. Alternatively, **5** and **6** can be generated by action of the corresponding Ni complexes on the neutral cluster $[Fe_4S_4(Stip)_2L_2]$ where the neutral ligands are displaced. The bidentate coordination mode of the Ni complexes to the Fe_4S_4 core of **3**, upon substitution of the iodide ligands by thiolates, changes to unidentate in **5**. The S_4 coordination set in **6** leads to an unsymmetrically bidentate binding of the Ni complexes. As demonstrated by ^{1}H-NMR spectroscopy, **3**, **5**, and **6** retain their bridged structures in solution. However, the spectra of **5** and **6** can be interpreted in terms of a symmetrically bidentate coordination of both Fe_4S_4-bound Ni complex fragments, which is in contrast to the unidentate (**5**) or unsymmetrically bidentate (**6**) binding observed in the solid state.

(iii) The Ni coordination spheres of thiolate-bridged assemblies **3**, **5**, and **6** exhibit structural features that are similar to the active centers of nickel−CO dehydrogenases from *C. thermoaceticum* and *R. rubrum*. Although the nickel content in the heterometallic clusters differs from that of the proposed substrate binding sites A and C in Ni−CODH/ACS, the structures of **3**, **5**, and **6** represent the first synthetically available examples of the Ni(μ_2-SR)$[Fe_4S_4]$ motif.

(iv) As shown by cyclic voltammetry, **5** can exist in four different redox states in dichloromethane solution. According to a tentative assignment, the three more reduced species correspond to different $[Fe_4S_4]^{n+}$ oxidation states (ranging from $n = 1$ to $n = 3$), whereas the most oxidized species seems to consist of an $[Fe_4S_4]^{3+}$ cluster and one Ni(III) center. However, the most reduced cluster could also be an $[Fe_4S_4]^{2+}$-Ni(II)Ni(I) species.

Acknowledgment. This research was supported by the Deutsche Forschungsgemeinschaft and the BMBF. We thank Dr. H. Strasdeit for helpful comments on the paper.

Supporting Information Available: Tables giving a complete list of atomic coordinates and anisotropic atomic displacement parameters of all non-hydrogen atoms (12 pages). See any current masthead page for ordering and Internet access instructions.

JA970194R

(49) Reversible redox processes for tetrathiolato-substituted Fe_4S_4 clusters usually are one-electron processes. See ref 40.

(50) Okuno, Y.; Uoto, K.; Yonemitsu, O.; Tomohiro, T. *J. Chem. Soc., Chem. Commun.* **1987**, 1018.

(51) This derivative is available by the following reaction sequence. 1,3-Diaminopropane was reacted with 2 equiv of benzoyl chloride. $LiAlH_4$ reduction leads to 1,3-bis(*N*-benzylamino)propane, which was treated with 2 equiv of ethylene sulfide in toluene. Reaction of the resulting $BenzN_2S_2H_2$ ligand with nickel(II) acetylacetonate in THF solution affords [Ni($BenzN_2S_2$)], which gives $[\{Ni(BenzN_2S_2)\}_2Fe_4S_4I_2]$ by reaction with $[Fe_4S_4I_4]^{2-}$ in CH_3CN.

(52) Nicholson, R. S. *Anal. Chem.* **1966**, *38*, 1406.